CSCanada
Advances in Petroleum Exploration and Development
Vol. 9, No. 2, 2015, pp. 98-102
DOI:10.3968/6918

ISSN 1925-542X [Print]
ISSN 1925-5438 [Online]
www.cscanada.net
www.cscanada.org

Investigation of the Factors Influencing Volume Fracturing of Tight Reservoir by Using Numerical Simulation

LIU Zhenyu[a],[b],*; ZHU Qianqian[a],[b]; WANG Huzhen[a],[b]; HE Jinbao[c]; LAN Xue[d]

[a] College of Petroleum Engineering, Northeast Petroleum University, Daqing, China.
[b] Key Laboratory Reservoir Stimulation, CNPC, Daqing, China.
[c] Instrument Research Institute of Drilling Technology Research Institute, China Petroleum, Panjin, China.
[d] Jilin Oilfield Exploration and Development Institute, China Petroleum, Songyuan, China.
*Corresponding author.

Supported by Heilongjiang Province Natural Science Foundation (A201201).

Received 23 April 2015; accepted 5 June 2015
Published online 30 June 2015

Abstract
Based on finite element method, a complex fracture model of volume fracturing has been established for tight oil in this paper, which achieves the actual description of complex fractures. For water injection conditions, the volume of fractures network after fractured which considered the influence of fracture segment was analyzed by using numerical simulation. By comparing and analyzing the simulation results, the most optimal fracture segment is 10. The research results provide a theoretical basis for the optimized design of volume fracturing in tight oil.

Key words: Tight oil; Volume fracturing; Numerical simulation; Finite element method

Liu, Z. Y., Zhu, Q. Q., Wang, H. Z., He, J. B., & Lan, X. (2015). Investigation of the factors influencing volume fracturing of tight reservoir by using numerical simulation. *Advances in Petroleum Exploration and Development*, *9*(2), 98-102. Available from: URL: http://www.cscanada.net/index.php/aped/article/view/6918
DOI: http://dx.doi.org/10.3968/6918

INTRODUCTION
With the increasing size of the proven reserves and the continuous development in the tight oil reservoirs, there is an increasing focus on reasonable and effective means of development. Tight oil reservoirs have the characteristics of low permeability, filtrational resistance, and poor connectedness and so on, it is difficult to meet the needs of economic development[1]. It is hard to achieve the expected stimulation effect only on the traditional single fracturing, because of the poor supply ability from the matrix to fracture in the tight oil reservoirs. Volume stimulating to reservoir, achieving the "short distance" from matrix to fracture because of producing fracture network[2-4]. Therefore, proposing volume fracturing technology to increase oil or gas production, this technology is suitable for low porosity, tight oil reservoir. According to the definition,volume fracturing form a complicated network fracture system which realized the comprehensive transformation of reservoir in three-dimensional direction, it has the vital significance to the exploitation of tight oil reservoirs[5-7].

1. BUILD MATHEMATICAL MODEL

1.1 Basic Assumptions
(a) Oil-water two-phase flow exists in reservoirs;
(b) Non-homogeneous anisotropic reservoir;
(c) Both micro-compressible fluid and rock;
(d) Considering the influence of capillary forces;
(e) Ignore the effects of gravity.

1.2 Differential Equations of Two-Phase Flow
Oil-water two-phase flow differential equation is:

$$\nabla \cdot [\rho_o \frac{K \cdot K_{ro}}{\mu_o} \nabla p_o] = \frac{\partial (\phi S_o \rho_o)}{\partial t}, \quad (1)$$

$$\nabla \cdot [\rho_w \frac{K \cdot K_{rw}}{\mu_w} \nabla p_w] = \frac{\partial (\phi S_w \rho_w)}{\partial t}. \quad (2)$$

Wherein: (a) the equation for the oil phase, (b) an aqueous phase equation.

In this equation, ρ represents fluid density, k represents permeability, k_r represents effective permeability, μ represents fluid viscosity, p represents pressure, ϕ represents porosity, S represents saturation, t represents time, o represents oil phase, w represents water phase.

1.3 Auxiliary Equation and Initial and Boundary Conditions

Auxiliary equation:

$$\begin{aligned} &\phi = \phi(p_o) \\ &p_c = p_c(S_w) = p_o - p_w . \\ &S_o + S_w = 1 \end{aligned} \quad (3)$$

In this equation, c represents capillary potential.

Initial conditions:

$$p_o|_{(t=0)}=p_{oi},\ S_w|_{t=0}=S_{wi} . \quad (4)$$

In this equation, oi represents the initial value of the oil phase, wi represents the initial value of the water phase.

Outer boundary condition:

$$\frac{\partial p_o}{\partial n}\Big|_{\Gamma 1} = 0 ,\ \frac{\partial S_w}{\partial n}\Big|_{\Gamma 2} = 0 . \quad (5)$$

In this equation, n represents the boundary outside the normal direction, Γ1, Γ2 represents closed boundary.

The boundary conditions (Wells border):

$$p_o|_{\Gamma 3} = p_{o1},\ S_w|_{\Gamma 4} = S_{w1} . \quad (6)$$

In this equation, Γ3 represents the constant pressure boundary, Γ4 represents the constant saturation boundary, ol represents the oil phase boundary value, wl represents the water phase boundary value.

1.4 Equation Derivation

The oil phase pressure equation

$$\nabla\cdot[(\frac{K\cdot K_{ro}}{\mu_o}+\frac{K\cdot K_{rw}}{\mu_w})\nabla p_o-\frac{K\cdot K_{rw}}{\mu_w}\nabla p_c(S_w)]+\frac{q_o}{\rho_o}+\frac{q_w}{\rho_w}=\phi C_t\frac{\partial p}{\partial t} . \quad (7)$$

The aqueous phase saturation equation:

$$\nabla\cdot(\frac{K\cdot K_{rw}}{\mu_w}\nabla p_o-\frac{K\cdot K_{rw}}{\mu_w}\nabla p_c^{\,n+1}(S_w))+\frac{q_w}{\rho_w}=\phi\frac{\partial S_w}{\partial t} . \quad (8)$$

Set shape function vector:

$$N = (N_1, N_2, ...N_n). \quad (9)$$

Trial solution for the oil phase pressure:

$$\tilde{p} = \sum_{i=1}^{n} N_i p_i . \quad (10)$$

Coordinates within the unit:

$$x = \sum_{i=1}^{n} N_i x_i ,\ y = \sum_{i=1}^{n} N_i y_i . \quad (11)$$

Can be obtained by derivation, the oil phase pressure finite element equilibrium equation:

$$K_{ep}P + C_{ep}\frac{\partial P}{\partial t} = F_{ep}. \quad (12)$$

In this equation, K represents the total stiffness matrix, C represents the total mass matrix, F represents the total load vector, ep represents pressure field.

Similarly, we can get the water phase saturation finite elements equilibrium equations:

$$C_{es}\frac{\partial S}{\partial t} + K_{es}S = F_{es} . \quad (13)$$

In this equation, es represents saturation field.

2. CASE STUDY

2.1 Simulation Area and Mesh Generation

After transforming the volume fracturing, it forms a complex network, and the permeability of the transformed area is improved. For easy simulated calculation, the transformed seam network is processed into two parts sewn main seam and the transformation of high permeability area, as shown in Figure 1. The width of transformed region is on the basis of micro-seismic monitoring result, and the permeability rate of this region is determined by history matching of single well.

The injection intensity of water injection wells at both ends of the horizontal section is 1 m^3/(m·d), and the middle wells' injection intensity on the segment is 0.8 m^3/(m·d). Well dimension is 700 m × 1,100 m, and horizontal length is 800m. We simulate separately different results of fracture number, different end seam length program, of which number 10, cluster 2, 150 m-half-length mesh generation is shown in Figure 2.

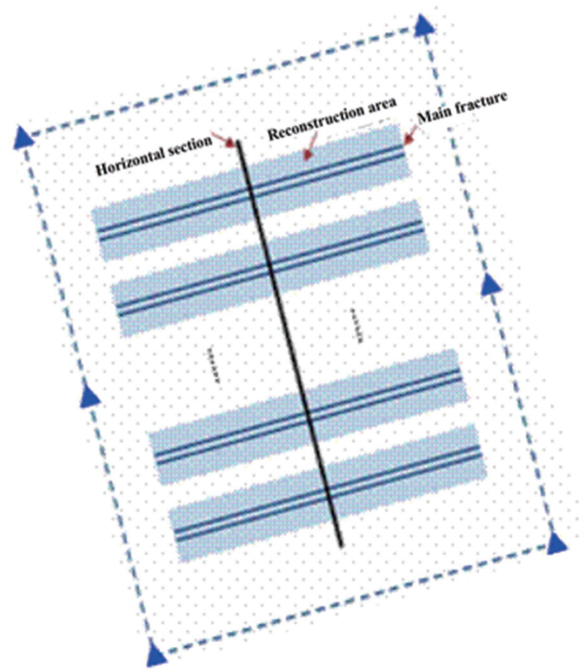

Figure 1
Schematic Simulation Area

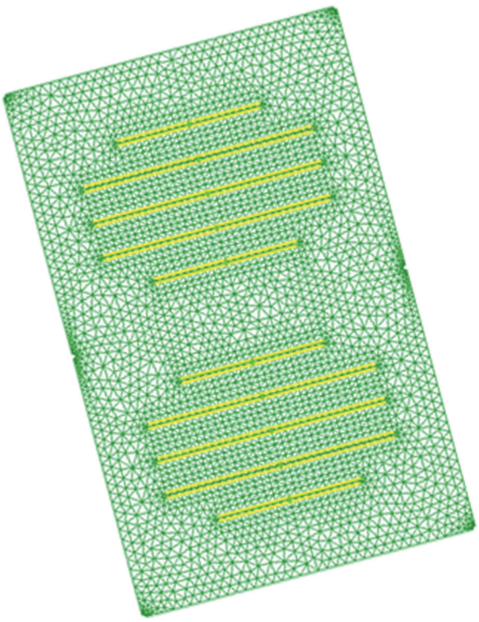

Figure 2
Meshing Figure

2.2 Calculation Parameters

Calculation Parameters Table Test Block Zhuang 230 well area are shown in Table 1.

Table 1
Zhuang 230 Well Area Calculation Parameters

Parameters	Value	Parameters	Value
The viscosity of initial oil in place (mPa·s)	1.5	Porosity	0.115
Oil volume factor	1.293	Initial formation pressure (MPa)	16.21
Formation permeability of gas survey (10^{-3} μm^2)	0.29	Oil well bottom pressure (MPa)	6.5
Formation effective thickness (m)	16.5	Fracture capacity (μm^2·cm)	20

2.3 Law of Impact of the Segments Number on the Volume Fracturing Effect

Under the conditions in horizontal length 800 m and segment clusters 2, we respectively simulate 4 scenarios of segment number. The number of segments of different scenarios are shown in Table 2. The ends fracture half length is taken as 180 m, Central taken as 240 m.

Table 2
Sections of the Scenario Table

Scenario	Scenario 1	Scenario 2	Scenario 3	Scenario 4
Number of segments	4	6	8	10

Figure 3 shows the dynamic curve of daily oil production in different segments of the number of scenarios, Figure 4 shows the dynamic curve of the moisture content of different number of segments. As can be seen from the figure, about half of a year ago, daily oil production decreased gradually, after about half of a year, daily oil production began to increase, about four years daily oil production began to decline rapidly, and the more the number of segments, the higher daily oil production. The water breakthrough time at different program segments is about 3 years. At the same time, the fewer the number of segments corresponding to the higher water content ratio, at 15 years, the number of programs in four segments of the water content ratio is not difference.

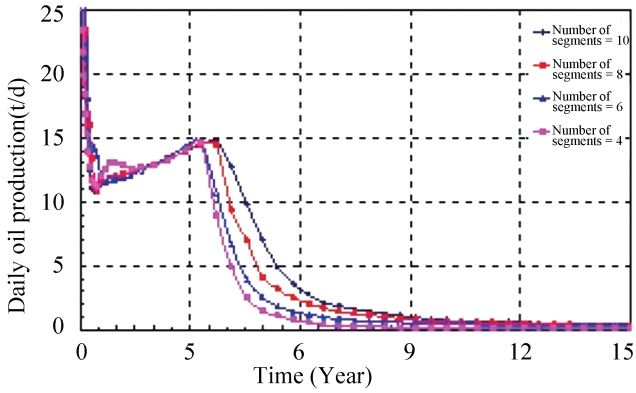

Figure 3
The Number of Different Segments of Daily Oil Production Scheme Dynamic Curve

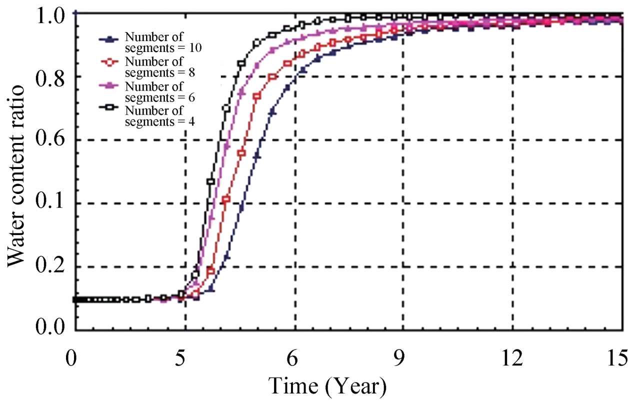

Figure 4
The Moisture Content of the Different Sections of the Dynamic Curve of the Number of Programs

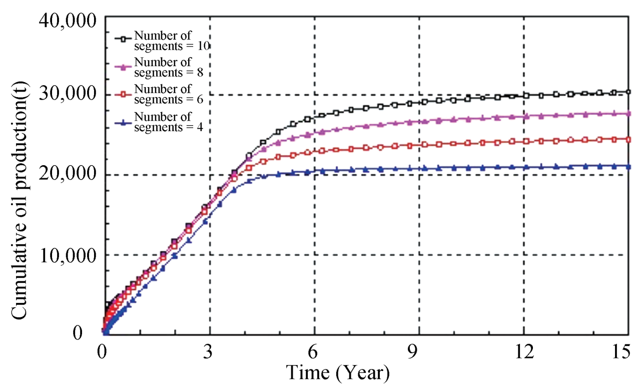

Figure 5
Different Number of Segments Cumulative Oil Production Dynamic Curve

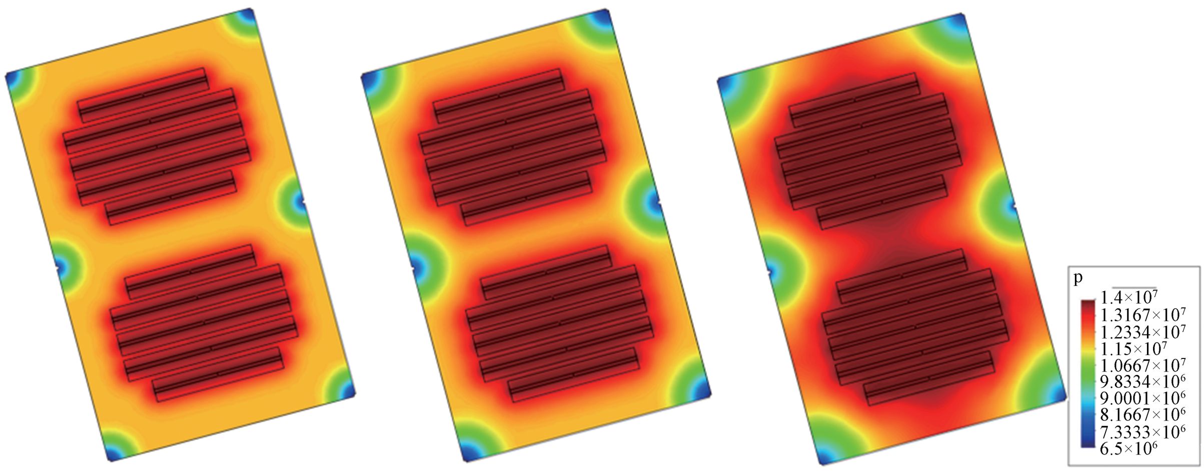

(a) 1 month (b) 3 months (c) 15 years

Figure 6
10 Paragraph and 2 Clusters (Horizontal Section Is 800 m) Pressure Distribution at Different Times

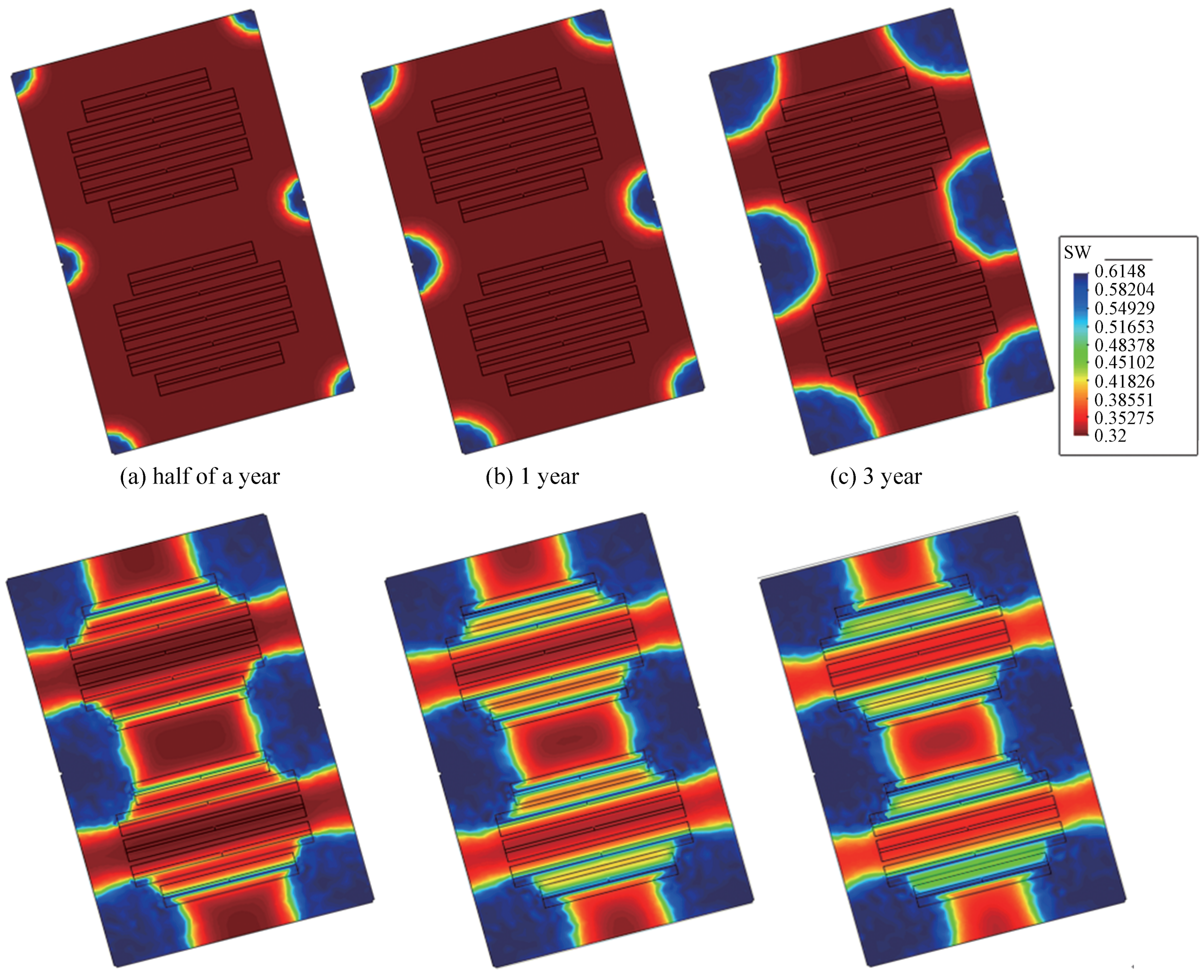

(a) half of a year (b) 1 year (c) 3 year

(a) 6 years (b) 10 years (c) 15 years

Figure 7
10 Paragraph and 2 Clusters (Horizontal Section Is 800 m) Saturation Distribution at Different Times

Table 3
Comparison of Different Number of Segments Cumulative Oil Production at the 15th Year

Number of segments	4	6	8	10
Cumulative oil production (t)	21,195	24,526	27,802	30,445
Increase the amount of in turn (t)		3,331	3,276	2,643
Increase the proportion in turn (%)		15.71	13.36	9.51

Figure 5 is a curve of the cumulative crude output. It can be seen that the more segments there are, the higher cumulative oil production will be. But with the increase in the number of segments, the rate of increase of the cumulative oil production becomes smaller. The comparative date of cumulative oil production for 15 years is in Table 3. As can be seen from the table, the cumulative oil production of 6 segments increased 3,331 t more than four segments, a 15.71 percent increase, 8 segments of the cumulative oil production increased by 3,273 t than six segments, improved by 13.36%, cumulative oil production of 10 segments increased by 2,643 t than 8 segments, a 9.51% increase. Studies show that: Under the current calculation conditions, taking the number of 10 segment is optimal.

Seven-spot horizontal section is 800 m, 10 segments and 2 clusters at different times of the pressure distribution shown in Figure 6.

Seven-spot horizontal section is 800 m, 10 segments and 2 clusters at different times of saturation distribution shown in Figure 7. As can be seen from the figure, the fracture farther from the wells is still not water breakthrough a lot at the 15th year.

CONCLUSION

(a) This paper established a complex fracture model dense reservoir of hydraulic fracturing based on finite element method, achieves the approximately real description of compact reservoir volume fracturing complex fractures, based on the numerical simulation results, the impact of the law of the number of segments developed fractures and end sewing length of fracturing effect has been worked out.

(b) The numerical results show that under seven-spot water injection conditions, the length of the horizontal section is 800 m, when two clusters of fractures within the segment, in order to achieve optimum cumulative oil production, take 10 as the number of segments.

REFERENCES

[1] Wang, H., & Wang, Q. (2012). Volume fracturing in the development and application of ultra-low permeability reservoirs. *China Petroleum and Chemical Standards and Quality*, (2), 143.

[2] Wang, W., Zhao, G., & Su, Y. (2013). Dense reservoir volume fracturing technology. *Xinjiang Petroleum Geology*, *32*(3), 345-348.

[3] Liu, Z., Zheng, X., & Zhang, Y. (2006). Security can be based on dynamic analysis of fractured wells producing artificial finite element method. *Daqing Petroleum Institute*, *30*(2), 30-34.

[4] Cai, T. (2013). *Volume numerical simulation of low permeability reservoir fracturing research* (Doctoral dissertation). Northeast Petroleum University, Daqing, China.

[5] Li, Y., Wei, C., Qin, G., Li, M., & Luo, K. (2013, March). *Numerical simulation of hydraulically induced fracture network propagation in shale formation*. Paper presented at International Petroleum Technology Conference, Beijing, China.

[6] Spencer, R. J., Pedersen, P. K., & Clarkson, C. R. (2011). Shale gas: Part 5–shale gas vs. tight gas vs. conventional gas. *Canadian Society of Petroleum Geologists Reservoir Magazine*, (1), 25-30.

[7] Rahmanian, M., Solano, N., & Aguilera, R. (2010, May). *Storage and output flow from shale and tight gas reservoirs*. Paper presented at the SPE Western Regional Meeting, Anaheim, California, USA.

